

# Geochemical and isotopic composition of groundwater in the Complex Terminal aquifer in southwestern Tunisia, with emphasis on the mixing by vertical leakage

Meriem Tarki · Lassaad Dassi · Younes Hamed ·  
Younes Jedoui

Received: 28 September 2009 / Accepted: 26 October 2010 / Published online: 11 November 2010  
© Springer-Verlag 2010

**Abstract** The Complex Terminal (CT) confined aquifer of the Djerid basin, southwestern Tunisia, was studied using major ion concentrations and stable isotope contents in order to (1) investigate the changes on its hydrodynamic functioning due to the long-term over-pumping and the large-scale flood irrigation practices, (2) determine the principal mineralization processes of its fossil groundwater, and (3) examine the mode of recharge of this aquifer and whether it contains part of modern hydrological regime. The observed geochemical patterns indicated that the main mineralization processes affecting the CT groundwater water/rock interactions and mixing. The native  $\text{Na} > \text{Cl}$  and  $\text{Cl} > \text{SO}_4 > \text{Ca} > \text{Na}$  waters, resulting from the dissolution of halite and gypsum and from pyrite oxidation, interacted with those of the underlying and the overlying aquifers without changing their chemical facies. Stable isotope data provided evidences about upward and downward leakage into the CT aquifer and their relationships with anthropogenic activities. They demonstrated that

the long-term over-pumping of the CT aquifer, which contributed to the loss of its potentiometric pressure, favored the upward leakage of the artesian deep groundwater along parts of the major faults. Moreover, the large-scale flood irrigation practices in the oases domain, which ensured the recharge of the shallow water table by return flow, enhanced the downward leakage toward the CT aquifer.

**Keywords** Complex Terminal aquifer · Hydrochemistry · Stable isotopes · Water/rock interaction · Mixing · Upward and downward leakage

## Introduction

Over the past few years, there has been an increased awareness among water managers in Tunisia of the necessity to manage internationally shared groundwater resources in a concerted manner. These resources are often described as “fossil” aquifers, which comprise non-renewable groundwaters characterized by no appreciable modern recharge and very low natural flow and discharge rates. Such groundwaters are generally trapped in deep geologic formations, either because of physical isolation of the aquifer from sources of recharge, impermeability of overlying strata or paucity of recharge in an arid region.

The CT aquifer is an immense non-renewable groundwater reservoir shared between Algeria, Tunisia, and Libya with total surface area of about 350,000 km<sup>2</sup> (Belloumi and Matoussi 2006). Its groundwater, which constitutes an important and vital resource for more than 4 million people living in the Northwestern African neighboring nations (Wallin et al. 2005), is used essentially for agricultural practices and occasionally for domestic water supplies.

---

M. Tarki · L. Dassi (✉) · Y. Jedoui  
Unité des Recherche Hydro-sciences Appliquées,  
ISSTE, 6072 Gabès, Tunisia  
e-mail: lassaad@geologist.com

M. Tarki  
e-mail: tarkimeriem@gmail.com

Y. Jedoui  
e-mail: younes.jedoui@issteg.rnu.tn

L. Dassi · Y. Hamed  
Département des Sciences de la Terre,  
Faculté des Sciences de Gabès, 6072 Gabès, Tunisia  
e-mail: hamed\_younes@yahoo.fr

Y. Hamed  
Laboratoire Eau-Energie-Environnement,  
ENIS, 3038 Sfax, Tunisia

However, this resource is subject to increased exploitation and may be severely stressed if not managed properly as witnessed already by declining water level. In 2000, the CT aquifer in Northwestern Sahara provided an estimated volume of about 1.4 billion m<sup>3</sup> (Horriche 2004) for fresh-water supply, agriculture, and other purposes including tourism.

In the Djerid basin, southwestern Tunisia, the increasing groundwater withdrawal in the CT aquifer during the past three decades has contributed to widespread changes in its piezometric head, i.e., lost of the original artesian condition. In order to make appropriate decisions for the sustainable management of this water resource, the needs increase for more precise hydrogeological data to help refine management decisions on water use. Several studies have been carried out to provide a basis for the characterization of the geology and the hydrogeology of the basin (e.g. Cornet 1964; Bel and Demargne 1966; ERESS 1972; Pallas 1980; BGS 1997; SASS 2002). Over the past two decades, numerous isotope investigations have been carried out with the assistance of the IAEA to assess the groundwater resource potential in the Djerid Basin. These studies indicated that for most of the groundwater from CT the oxygen-18 and deuterium isotope contents are depleted compared to those of the modern rainfall. This would suggest that the modern rainfall is not affecting this groundwater, although some sources for active recharge have been identified particularly during years of exceptional rainfall.

Although the available isotopic data have already provided useful information for the understanding of the general functioning and hydrodynamic of the CT main aquifer in the Djerid basin, there still remain important ambiguities such as the possibility of its modern recharge,

the influence of the over-pumping and increasing irrigation practices on its flow patterns and on its interrelations with the underlying and the overlying aquifers.

## Geological and hydrogeological background

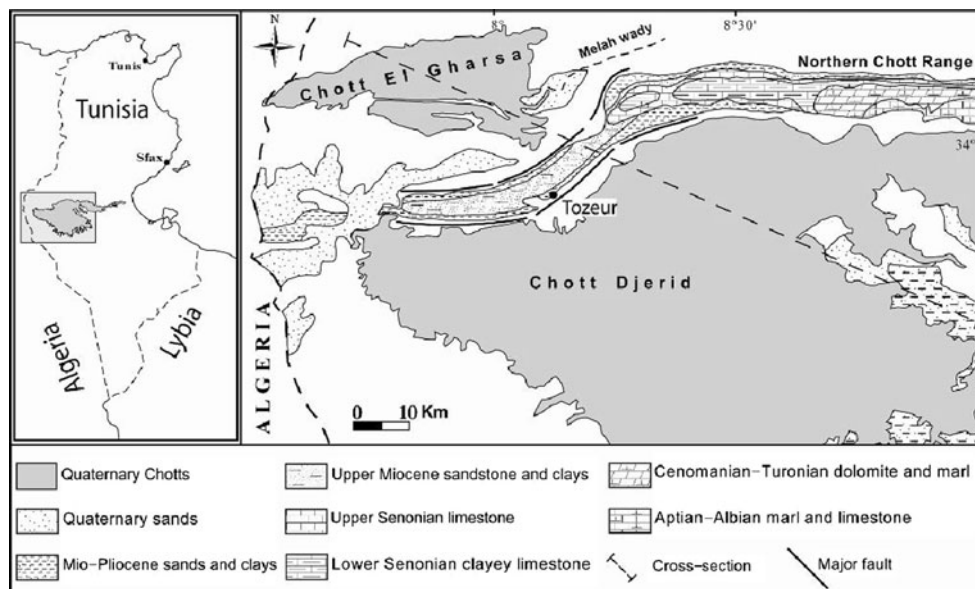
### Location and physical characteristics

The Djerid basin, which covers about 5,000 km<sup>2</sup> area of southwestern Tunisia, is bordered by the latitudes 33°–34° north and the longitudes 7°30′–8°30′ east (Fig. 1). It is limited in the west by the Algerian frontier, in the east by the mountains of the Northern Chotts Range, in the north and in the south by the continental depressions of Chott el Gharsa and Chott Djerid, respectively. This basin is characterized by an arid climate with a mean annual precipitation and potential evapotranspiration of 100 and 1,700 mm, respectively (Kamel et al. 2005). The surface drainage network is insignificant. However, important runoff events occurring particularly during years of exceptional rainfall can engender some non-perennial streams known locally as “wadis.” These wadis collect surface runoff from the surrounding highlands and bring them to the continental depressions of Chott el Gharsa and Chott Djerid, which constitute the natural discharge areas of the basin.

### Geology

Several studies indicated that the geological formations present in the Djerid basin date from the Jurassic to the Quaternary. The outcropping sediments range from the Neogene to the Upper Cretaceous (Fig. 1). However, in the

**Fig. 1** Geological map of the study area



depth there is a succession of the different sedimentary units extending until the Jurassic age.

From a tectonic point of view, the Djerid basin represents a transitional zone between the Tunisian Atlasic Chain in the north and the Saharan platform in the south. The regional structural studies highlight the existence of two east-west major faults, which contributed to the uplifting of the Draa Djerid anticline, constituting thus the horst of Tozeur or the so-called “Tozeur ridge” (Zargouni 1986; Mamou 1990; Abidi 1993; Moumni 2001). These transversal faults, which are located between the two continental depressions, extend in the whole basin from the town of Hazoua in the west to the town of Hamma in the east, where they disappear in the foothill zone of the northern Chott Range. Other geophysical explorations mentioned the presence of two N–S geophysical faults extending longitudinally in the regions of Hamma and Hazoua across the Draa Djerid anticline (Zargouni 1986).

Hydrogeology

The Djerid basin encompasses three aquifers: the deep Continental Intercalaire (CI), the intermediate Complex

Terminal (CT) and the shallow Plio-Quaternary (PQ) (Fig. 2). The CI and the PQ aquifers are slightly solicited in this basin because of the relatively high depth, ranging between 1,600 and 2,300 m, of the first aquifer and the low groundwater potentiality of the second. Therefore, the emphasis of this study concerns only the CT aquifer because of its high potentiality, in relation with its large spatial extension, and the relatively good quality of its groundwater.

In the Djerid basin, the CT aquifer, which has an average thickness of about 180 m, is hosted in the Tertiary sands and clayey sands of the Beglia Formation (Burdigalian-Langhian). It lies unconformably and indiscriminately over the Upper Senonian (Canpanian) of the Berda Formation, which constitutes the CT aquifer in the Nefzaoua neighboring basin. The basement of the CT, in the Djerid as well as in the Nefzaoua region, is constituted by the Lower Senonian (Santonian-Coniacian) shales, calcareous mudstone, and anhydrite of the Aleg Formation.

From structural point of view, the CT aquifer is constituted by a large SW–NE syncline (Fig. 2) in the center of which there is a relatively small anticlinal structure (Rouatbi 1967). This anticline is crossed and uplifted in the

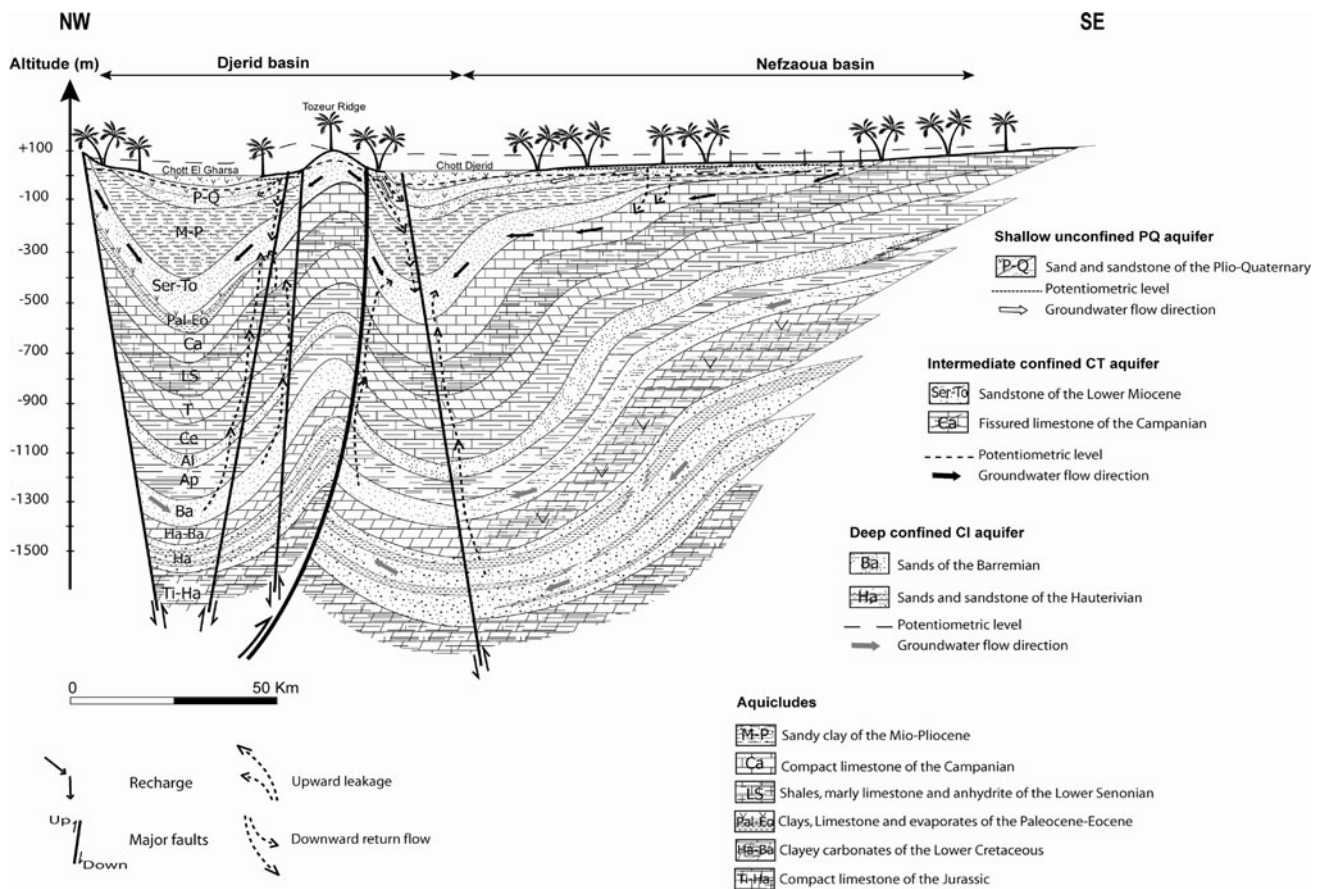


Fig. 2 Hydrogeological cross-section of the Djerid basin

central part of the basin by the two major faults that limit the “Tozeur ridge”. Therefore, the CT aquifer, which dips normally to the depth from the borders to the center of the basin, was firstly brought to the surface and then completely eroded between the two mentioned major faults.

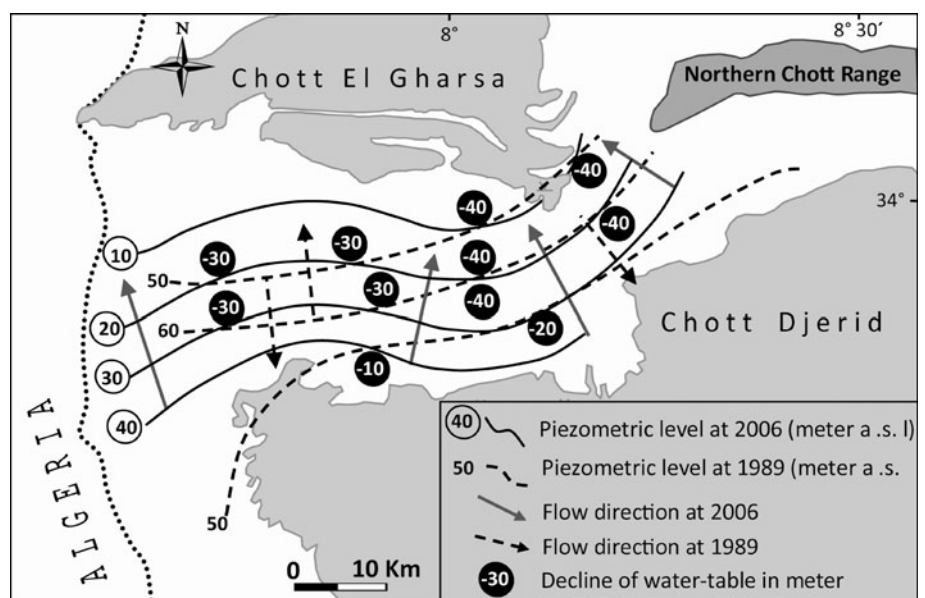
Hydrogeologically, the tectonic activity has played a major role in the hydrodynamic functioning of the CT aquifer. The compartmentalization of this groundwater reservoir has contributed to the creation of two independent and isolated hydrogeologic compartments located to the north and to the south from the so-called “Tozeur ridge”. In fact, the piezometric map of the 1980s (Mamou 1990) showed two opposites major S–N and N–S flow directions, which diverge from the “Tozeur ridge” to the discharge depressions of Chott el Gharsa and Chott Djerid, respectively (Fig. 3). These opposite flow directions indicated that the CT outcrops on both sides of the “Tozeur ridge” constituted the main recharge area of the CT aquifer in the basin. However, the latest piezometric map, established within the present study at 2006 (Fig. 3), shows several changes in the CT groundwater flow patterns. The two flow directions diverging from the “Tozeur ridge” have been completely disappeared and replaced by other major flows coming from the south and from the southeast towards the Chott el Gharsa depression. These new flow directions highlight the presence of two recharge components in relation with the aquifer outcrops in the Grand Erg Oriental and in the Dahar Mountain. On the other hand, the extinction of the flow directions coming from the “Tozeur ridge” can be explained by the severe climatic condition that characterized the south of Tunisia during the last two decades. Another potentiometric change appears from the comparison of the two maps (Fig. 3). It is the remarkable

decline of the piezometric level that ranges between 10 and 40 m indicating the influence of the long-term over-pumping of the CT groundwater in the Djerid basin. This over-pumping, which is in relation with the increasing number of the CT boreholes in response to the large extension of the agricultural areas, has contributed to several deleterious and irreversible consequences including the drying of all springs and the water quality degradation, presumably due to the mixing with the overlying and/or the underling groundwaters.

### Sampling and analysis

Water samples for laboratory analyses were collected during December 2006. A total of 38 groundwater samples was collected from the CT wells with depths ranging between 150 and 800 m (Fig. 4). Prior to sampling, all wells were purged in order to remove the stagnant portion and collect representative water samples. Temperature, pH, and electrical conductivity (EC) of the discharge water were measured using a Consort C535 multi-parameter analyzer. After that, sample bottles were filled and kept in a refrigerator upon collection. The geochemical analysis were carried out in the “Laboratoire de Radio-Analyses et Environnement” of the “Ecole Nationale d’Ingenieurs de Sfax” in Tunisia, using a Dionex DX 100 ion chromatograph equipped with a CS12 and an AS14A-SC Ion Pac columns and an AS-40 auto-sampler. The saturation with respect to same minerals and the partial pressure of carbon dioxide ( $p\text{CO}_2$ ) of all sampled water were determined using the WateqF subroutine program (Plummer et al. 1992).

**Fig. 3** Piezometric map of the Complex Terminal water table at 1989 and 2006 showing the evolution of the water level



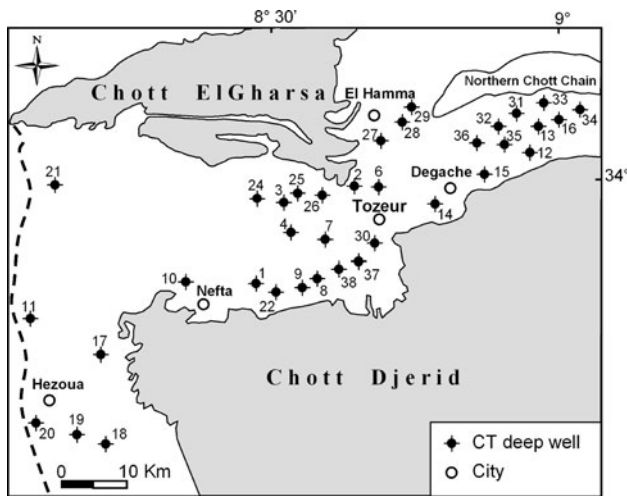


**Fig. 4** Location of sampled boreholes

Stable isotopes of oxygen and hydrogen were determined using isotope ratio mass spectrometry. The  $\delta^{18}\text{O}$  values in samples were analyzed via equilibration with  $\text{CO}_2$  at  $25^\circ\text{C}$  for 24 h (Epstein and Mayeda 1953) and for the  $\delta^2\text{H}$  values via reaction with Cr at  $850^\circ\text{C}$  (Coleman et al. 1982). Both  $\delta^{18}\text{O}$  and  $\delta^2\text{H}$  values were determined relative to internal standards that were calibrated using IAEA SMOW standards. Data were normalized following Coplen (1988) and were expressed relative to vs. SMOW. Samples were measured at least in duplicates and the precision of the analytical measures is  $\pm 0.1\%$  for  $\delta^{18}\text{O}$  and  $\pm 1\%$  for  $\delta^2\text{H}$ .

## Results and discussion

### Geochemical evolution and mineralization processes

#### *In situ measurements interpretation*

The results of geochemical analysis, in situ measurements, saturation index (SI) and partial pressure of  $\text{CO}_2$  ( $p\text{CO}_2$ ) are shown in Table 1. Groundwater well-head temperatures varied, in a relatively wide range, between 26 and  $37.4^\circ\text{C}$ . However, as it was expected, no good correlation was observed between water temperatures and the screened depth intervals. This may indicate that the CT groundwater receives some leakage from the overlying and/or underlying aquifers. The pH of the groundwater ranged between 6 and 7 (Table 1), an indication that the dissolved carbonates were predominantly in the  $\text{HCO}_3$  form (Adams et al. 2001). The higher  $p\text{CO}_2$  in the infiltrating water (ranging between  $1.32 \times 10^{-2}$  and  $5.38 \times 10^{-2}$  atm) compared to the precipitation  $p\text{CO}_2$  of  $10^{-3.5}$  atm suggested that the water gained  $\text{CO}_2$  from root respiration and the decay of soil

organic matter. Subsequently, an increase in  $p\text{CO}_2$  caused a drop in pH (Fig. 5). The EC and TDS were not homogeneous (Table 1), indicating that the CT waters differed considerably probably due to the mixing by vertical leakage with the overlying and/or the underlying aquifers with distinct hydrochemical composition.

#### *Water types*

The plot of the CT groundwater samples in the Chadha (1999) diagram (Fig. 6) showed two groups; the alkaline earths-rich group (group A) and the alkali metals-rich group (group B). The first group, which comprised the majority of the analyzed samples, showed that the alkaline earths ( $\text{Ca} + \text{Mg}$ ) exceeded the alkali metals ( $\text{Na} + \text{K}$ ) and that the strong acids ( $\text{Cl} + \text{SO}_4$ ) exceeded the weak acid ( $\text{HCO}_3$ ). The second group, which included only three samples, revealed that ( $\text{Na} + \text{K}$ ) was superior to ( $\text{Ca} + \text{Mg}$ ) and that the strong acids ( $\text{Cl} + \text{SO}_4$ ) exceeded the weak acid ( $\text{HCO}_3$ ).

Based on their chemical composition, group B plots on the field of the Na–Cl water type and group A plots in the field of Ca–Mg– $\text{SO}_4$ /Ca–Mg–Cl water type. However, among the major cations, calcium (with a mean value of 39%) predominated sodium (mean value 36%), whereas, among the anions, chloride (with mean value of 51%) predominated sulfates (with a mean value of 44%). Consequently, the chemical facies of the CT groundwater showed two main water types:  $\text{Na} > \text{Cl}$  and  $\text{Cl} > \text{SO}_4 > \text{Ca} > \text{Na}$ . The  $\text{Na} > \text{Cl}$  water type indicated the predominance of the halite dissolution. While, the  $\text{Cl} > \text{SO}_4 > \text{Ca} > \text{Na}$  water type indicated the coexistence of the dissolution of both halite and gypsum and the Ca–Na cation exchange. Indeed, this cation exchange diminished the concentration of Na and increased that of calcium, which augmented the saturation of groundwater with respect to Ca, contributing to the decrease of gypsum dissolution. This mechanism maintained the concentration of sulfates always inferior to that of chloride, a conservative element. Moreover, the consumption of the sodium throughout the cation exchange made the groundwater more undersaturated with respect to halite, leading to its further dissolution.

#### Major ions geochemistry and saturation states

Major reactive minerals in the CT aquifer of the Djerid basin are halite (NaCl), gypsum ( $\text{CaSO}_4 \cdot 2\text{H}_2\text{O}$ ) and/or anhydrite ( $\text{CaSO}_4$ ). The interactions of these minerals with waters largely define the chemical composition of groundwater. The computed SI values showed that groundwater in the CT aquifer was largely undersaturated with respect to halite ( $-6.08 \leq \text{SI} \leq -4.6$ ) and, to a lesser extent, with respect to anhydrite ( $-1.12 \leq \text{SI} \leq -0.28$ )

**Table 1** Chemical and isotopic data of the sampled CT boreholes

Borehole	Number	T (°C)	pH	pCO <sub>2</sub> (10 <sup>-2</sup> atm)	EC (μS/cm)	Screened interval (m)	Cl	SO <sub>4</sub>	HCO <sub>3</sub>	Na	K (mEq/l)	Mg	Ca	TDS (mg/l)	SI	Halite		δ <sup>18</sup> O vs. SMOW (‰)	δ <sup>2</sup> H
																Gypsum	Anhydrite		
Sif Lakdhar	1	31.1	6.71	6.71	2,053.1	532.5–624	22.2	21.7	2.4	20.3	1.3	10.3	14.5	2,933	-5.132	-0.483	-0.64	-4.185	-44.7
Chemsa 2bis	2	30.4	6.78	3.26	2,370.2	508–598	21.3	27.7	2.6	18.8	1.5	11.0	20.5	3,386	-5.19	-0.284	-0.448	-4.935	-48.3
Chabbat 3ter	3	30.2	6.72	3.26	2,370.2	545–672	20.9	27.4	2.6	18.9	1.5	9.1	19.7	3,386	-5.14	-0.275	-0.444	-4.855	-51.5
Moncef 3bis	4	31.6	6.39	5.38	2,270.8	561–633	16.1	23.8	2.4	19.2	1.4	11.7	21.8	3,244	-5.3	-0.312	-0.465	-5.03	-48.7
Chabbat 11bis	5	30	6.65	3.06	2,429	629–714	21.3	26.0	2.5	19.7	1.0	10.7	15.1	3,470	-5.164	-0.409	-0.577	-4.97	-50
Nelayet 3bis	6	32.5	6.8	2.67	2,501.1	268.5–324	26.3	25.3	2.8	17.7	1.5	10.8	27.9	3,573	-5.134	-0.214	-0.358	-4.915	-47.5
Mrah 15	7	30.6	6.5	4.86	3,038.7	512.5–578.5	46.6	19.7	3.0	28.1	1.3	16.3	28.9	4,341	-4.915	-0.357	-0.518	-3.92	-43.8
Mrah 2bis	8	32.4	6.8	2.32	1,906.8	509–606	20.3	19.7	2.6	15.8	1.1	9.9	18.8	2,724	-5.279	-0.415	-0.56	-3.98	-41.55
Mrah Ibis	9	32	6.8	2.1	1,988	602–672	15.0	25.2	2.4	17.2	0.7	9.8	15.4	2,840	-5.374	-0.396	-0.545	-4.555	-46.2
Nefta 4bis	10	30.5	6.57	3.37	3,539.9	401–486	47.5	32.3	2.5	23.0	1.5	22.4	35.8	5,057	-4.785	-0.126	-0.288	-5.05	-51.25
Mzara CT	11	32.4	6.66	3.29	2,220.4	323–361	23.7	23.4	2.7	17.2	1.0	11.0	20.3	3,172	-5.185	-0.344	-0.489	-4.81	-46.85
Cedada 8	12	36.5	6.74	2.54	1,847.3	551.3–585.9	24.9	12.7	2.3	16.8	0.6	9.5	14.1	2,639	-5.165	-0.074	-0.784	-5.815	-53.6
Cedada 10	13	35.4	6.82	2.07	1,309	524.5–559.9	15.9	10.8	2.2	12.9	0.6	7.0	8.0	1,870	-5.45	-0.881	-1.001	-5.94	-51.15
Ain torba	14	32.8	6.83	1.82	1,498	75–112	15.2	14.9	2.1	11.4	0.5	7.9	12.2	2,140	-5.529	-0.622	-0.764	-5.835	-49.9
Degache CT	15	30.5	6.8	1.88	1,635.2	98–155.4	20.7	12.4	2.1	19.2	0.9	8.3	9.8	2,336	-5.168	-0.791	-0.954	-5.35	-50.35
Dghoumes 4	16	34.8	6.82	1.88	3,171.7	550–620	53.9	17.9	2.3	30.6	1.5	16.5	28.7	4,531	-4.609	-0.412	-0.536	-5.91	-49.3
G.Jaballah	17	32	6.7	2.9	2,251.2	325–395	25.8	20.5	2.6	25.1	1.4	9.6	15.5	3,216	-4.981	-0.488	-0.637	-4.695	-47.3
Bir Roumi	18	27.8	6.51	4.48	2,300.2	287–341	20.8	25.3	2.8	15.8	1.2	11.7	23.6	3,286	-5.27	-0.259	-0.448	-5.045	-51.15
A.O. grissi	19	30.5	6.64	3.54	2,209.9	443–489	23.5	23.0	2.8	20.3	1.1	9.7	15.2	3,157	-5.108	-0.445	-0.608	-4.52	-47.55
Hazoua Ibis	20	32.4	6.65	3	2,212	443–489	25.2	20.4	2.4	21.0	1.4	9.1	20.4	3,160	-5.071	-0.386	-0.532	-4.69	-46.55
Htam CT	21	33.4	6.69	2.95	2,538.2	666–739	26.8	28.1	2.4	25.9	1.0	12.9	16.0	3,626	-4.973	-0.399	-0.502	-5.2	-50.55
Zaafra	22	33.7	6.76	2.25	2,564.8	612–672	20.7	32.4	2.3	21.2	0.9	13.8	21.7	3,664	-5.164	-0.233	-0.367	-6.175	-54.05
Ghardgoya	23	33	6.74	3.05	2,450	285–380	14.9	34.5	3.0	15.6	0.7	12.4	23.5	3,500	-5.435	-0.167	-0.307	-6.11	-53.9
Chabbat Ibis	24	30	6.8	1.32	2,387	603–754	24.4	26.3	3.1	18.4	1.2	10.2	24.0	3,410	-5.132	-0.239	-0.446	-	-
Chabbat 8	25	30.6	6.75	2.49	2,386.3	615–674	20.3	29.3	2.6	18.1	0.8	11.6	24.8	3,409	-5.231	-0.219	-0.381	-4.92	-47.7
Chabbat 13bis	26	33.6	6.7	2.34	2,430.4	492–536.5	20.8	29.9	2.3	19.0	1.2	11.1	24.3	3,472	-5.199	-0.201	-0.367	-5.04	-48.4
Hamma 16	27	33.6	6.7	2.65	2,072.7	156–220	19.9	18.3	2.3	14.5	1.1	8.7	17.6	2,961	-5.325	-0.453	-0.588	-4.48	-45.05
Hamma 7bis	28	30.8	6.67	2.53	3,895.5	117–202	44.9	38.3	2.4	25.0	1.1	18.5	47.7	5,565	-4.781	0.033	-0.126	-7.415	-51.2
Hamma 5bis	29	34.2	6.68	2.6	3,896.9	192–270	45.2	39.1	2.4	25.6	2.1	17.8	47.9	5,567	-4.776	0.035	-0.094	-7.345	-51.75
Tozeur 8	30	30	6.78	2.12	1,787.1	320–400	21.0	17.2	2.3	17.0	1.0	7.7	13.2	2,553	-5.22	-0.566	-0.734	-3.85	-43.6
Tazrarit Mtgne	31	34	6.68	2.91	3,887.8	245–403	67.9	19.4	2.7	49.3	2.9	13.1	24.2	5,554	-4.301	-0.452	-0.609	-	-
Tazrarit Ibis	32	32.6	6.85	1.66	3,000.2	49–91	51.0	16.8	2.2	29.6	2.0	16.6	20.9	4,286	-4.636	-0.531	-0.674	-6.04	-50.09
Dghmes Mtgne	33	27.6	6.7	2.03	3,341.8	635–696	83.3	25.2	2.1	27.8	1.6	26.8	28.4	4,774	-4.462	-0.329	-0.518	-	-
Dghoumes 2bis	34	35.4	6.7	2.57	3,371.2	680–785	65.3	15.9	2.4	30.2	0.9	21.1	29.1	4,816	-4.54	-0.483	-0.602	-4.07	-41.55

Table 1 continued

Borehole	Number	T (°C)	pH	pCO <sub>2</sub> (10 <sup>-2</sup> atm)	EC (µS/cm)	Screened interval (m)	Cl	SO <sub>4</sub>	HCO <sub>3</sub>	Na	K (mEq/l)	Mg	Ca	TDS (mg/l)	SI	Halite		δ <sup>18</sup> O vs. SMOW (‰)	δ <sup>2</sup> H
																Gypsum	Anhydrite		
Kriz	35	28	6.74	2.18	3,307.5	62–98	65.1	14.0	2.5	25.4	2.0	23.2	29.4	4,725	-4.596	-0.518	-0.704	-6.06	-47.94
El Horchani	36	31.6	6.75	2.27	8,13.4	285–322	7.8	7.4	2.1	5.7	0.6	6.0	5.0	1,162	-6.079	-1.127	-1.128	-	-
Chouchet	37	30	6.78	2.96	2,030	385–469	25.4	18.8	3.3	13.4	1.0	21.4	11.9	2,900	-5.254	-0.653	-0.82	-4.56	-42.9
Errached	38	31.1	6.83	2.11	1,960	376–478	25.5	18.9	2.6	13.4	1.4	19.8	10.6	2,800	-5.253	-0.686	-0.843	-	-

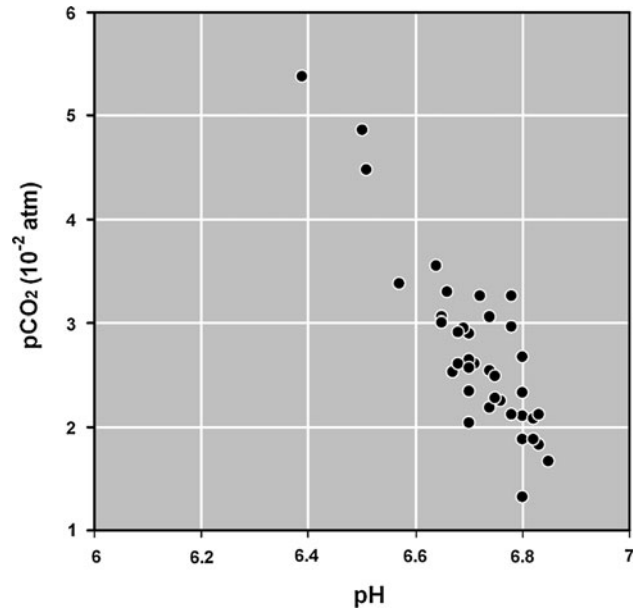


Fig. 5 pH/CO<sub>2</sub> relationship for sampled boreholes

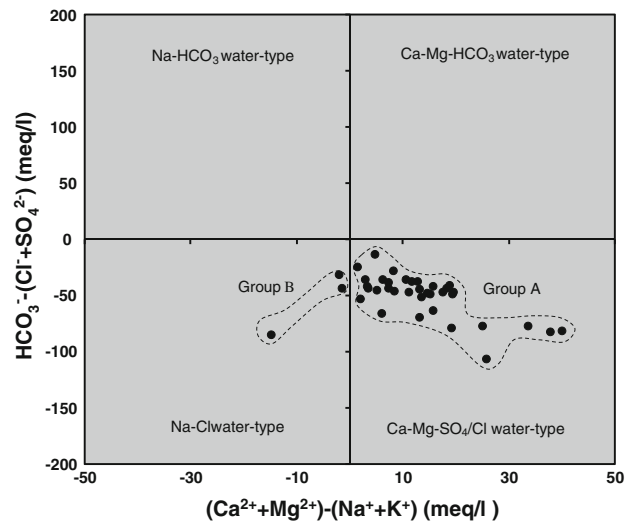


Fig. 6 Chadha diagram of the CT groundwater samples

and gypsum ( $-0.81 \leq SI \leq -0.07$ ), indicating possible dissolution of these minerals. These eventual dissolutions were confirmed by strong positive relationships of Na versus Cl and Ca versus SO<sub>4</sub> (Figs. 7, 8) as well as by the positive correlations between the SI of the referred dissolved minerals and some of ions resulting from each dissolution (Figs. 9, 10, 11). However, in the Na versus Cl Binary relationship, a remarkable deficit of Na was seen. The most probable explanation of this deficit was the contribution of Na in the cation-exchange reaction occurring between the Complex Terminal Na-rich water and the sediments, according to the equation:

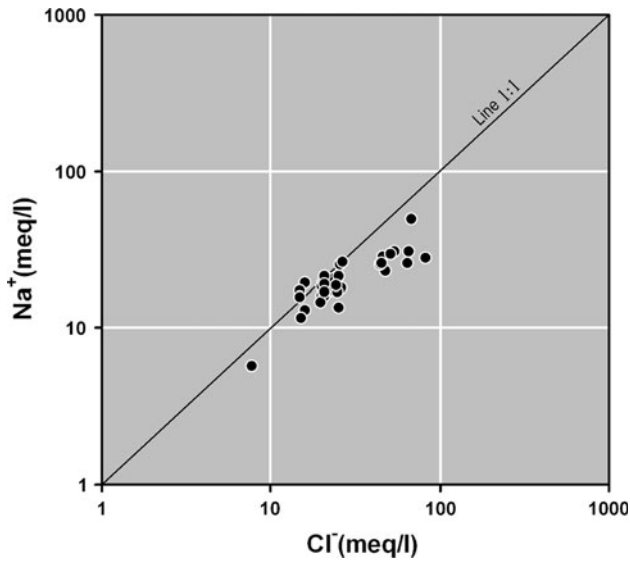


Fig. 7 Na versus Cl relationship for sampled boreholes

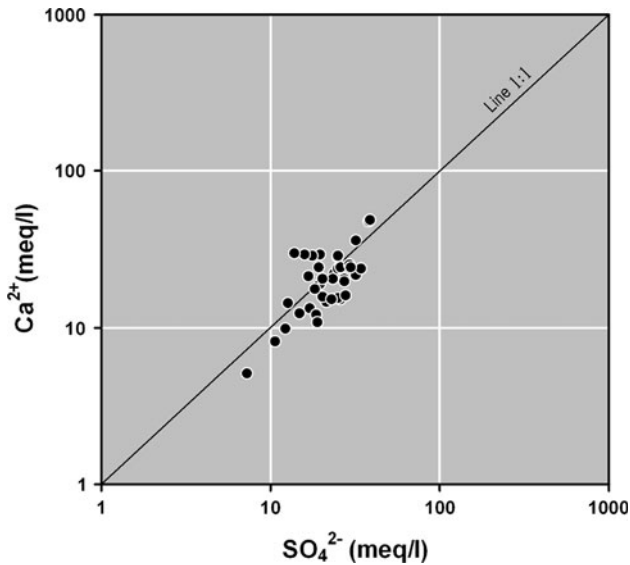
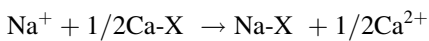


Fig. 8 Ca versus SO<sub>4</sub> relationship for sampled boreholes



where X indicates the sediment exchanger (Appelo and Postma 1993). Evidences of the cation-exchange reaction was provided by the Na/Cl versus Ca/(HCO<sub>3</sub> + SO<sub>4</sub>) relationship (Fig. 12), where the samples affected by this process plot in the field indicating the deficit of Na and the excess of Ca.

Another evidence of the predominance of the cation exchange was given by the Ca versus SO<sub>4</sub> plot (Fig. 8), where the samples showing an excess of calcium indicated its release into water to compensate the adsorption of sodium. While, samples exhibiting an excess of sulfates

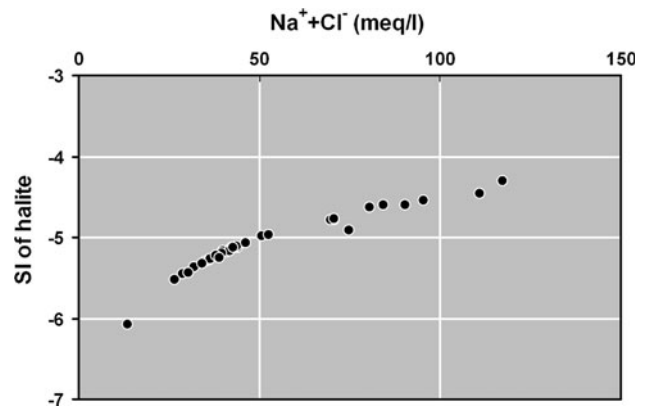


Fig. 9 (Na + Cl) versus SI (halite) relationship showing the dissolution of halite

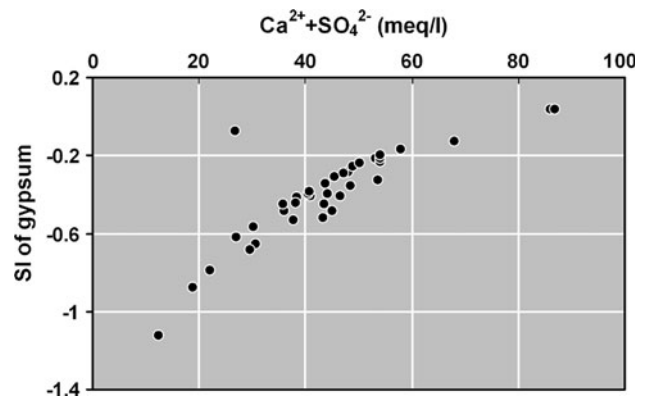


Fig. 10 (Ca + SO<sub>4</sub>) versus SI (gypsum) relationship showing the dissolution of gypsum

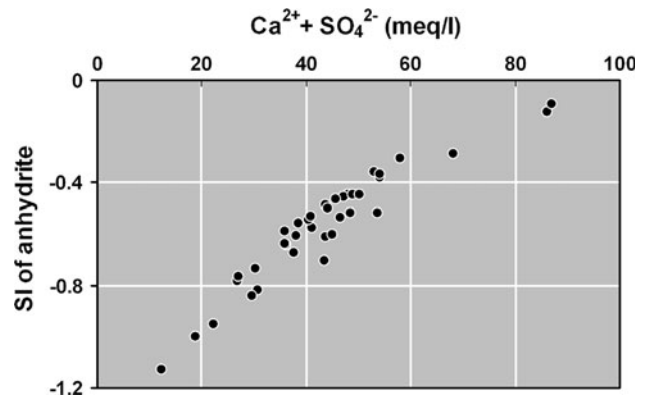
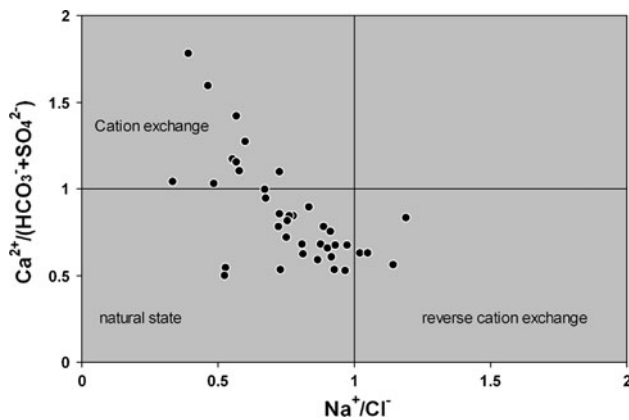


Fig. 11 (Ca + SO<sub>4</sub>) versus SI (anhydrite) relationship for sampled anhydrite

reflected a likely oxidizing environment of the CT aquifer, already evidenced by the presence of indirect indicators such as Fe (BGS 1997). In such an environment, it may be possible that pyrite, relatively abundant in the CT and





**Fig. 12** (Na/Cl) versus (Ca/(HCO<sub>3</sub> + SO<sub>4</sub>)) relationship showing the cation-exchange process

especially in the CI underlying aquifer, was subject to oxidation reactions.

Isotopic interpretation of groundwater pathways

*δ<sup>2</sup>H/δ<sup>18</sup>O diagram*

Oxygen and hydrogen isotope compositions for the investigated CT groundwater samples are represented in the conventional  $\delta^2\text{H}/\delta^{18}\text{O}$  diagram together (Fig. 13), with the Global Meteoric Water Line (GMWL) (Craig 1961), the Rocal Meteoric Water Line (RMWL) of the Sfax city located at about 200 km from the study area, and the so-called “Palaeo-Meteoric” Water Line (PMWL) (Sonntag et al. 1978). Additional data concerning the underlying (CI) and the overlying (PQ) aquifers were used, including the weighted mean values of stable isotope contents of CI (Edmunds et al. 2003) and PQ (Tarki 2008) groundwaters in Tunisia.

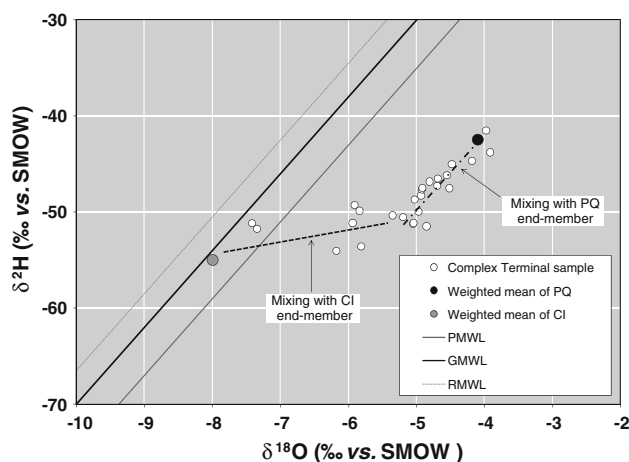


**Fig. 13**  $\delta^{18}\text{O}$  versus  $\delta^2\text{H}$  diagram for sampled boreholes

The  $\delta^{18}\text{O}$  and  $\delta^2\text{H}$  contents of the CT samples varied in a relatively wide range from  $-7.41$  to  $-3.92\text{‰}$  and from  $-54.1$  to  $-41.55\text{‰}$ , respectively. The weighted mean values of  $\delta^{18}\text{O}$  were  $-8\text{‰}$  for the CI and  $-4.1\text{‰}$  for the PQ. Those of  $\delta^2\text{H}$  are  $-55\text{‰}$  for the CI and  $-42.5\text{‰}$  for the PQ.

All CT samples lied below the three meteoric water lines, except for two samples lied between the GMWL and the PMWL. This indicated the old origin of the CT groundwaters in relation to their recharge during the paleoclimatic cooler regimes. Indeed, palaeowater stable isotope signatures in the Djerid basin, like all low-latitude semi-arid regions, are likely to be controlled more by precipitation amount and intensity than temperatures as in higher-latitude temperate regions (Clark and Fritz 1997). These paleowaters are characterized by an excess of deuterium of  $<10\%$  (Sadek and Abd El-Samie 2001; Edmunds et al. 2003) in contrast to the modern rainfall with a  $^2\text{H}$  excess of  $15\%$  representing the lower humidity caused by primary evaporation in the vapor source as it moves from the Atlantic region (Edmunds et al. 2003). Moreover, the fact that the CT groundwater lies well below the meteoric water lines also indicates that the evolution of air masses was different to the present-day with little or no primary evaporation and probably little upcoming from its Atlantic Ocean source region which was isotopically enriched as a result of ice-cap formation. On the other hand, the stable isotope results are also consistent with the those of carbon-14 (ERESS 1972; Gonfiantini et al. 1974; Fontes et al. 1983; Zouari et al. 1985; Mamou 1990; Zouari and Mamou 1992; Daoud 1995; Guendouz and Moulla 1996; Guendouz et al. 1997; Jeribi 1997; Zouari and Mamou 1998; Edmunds et al. 2003; Kamel et al. 2005; Kamel 2007), which indicate that the main recharge of the CT in southern Tunisia and Algeria occurred during the Late Pleistocene and the Early Holocene periods.

The CT samples scattered in a wide range of stable isotopes enrichment (especially for  $^{18}\text{O}$ ), and could be subdivided into two well-separated groups indicating probably distinct leakages from the underlying and the overlying aquifers. The first group, constituted by the deepest CT boreholes and by those located near the major faults, was characterized by the more depleted contents of  $\delta^{18}\text{O}$  and  $\delta^2\text{H}$ . The samples belonging to this group plot along an estimated mixing line extending towards the point representing the weighted mean of the CI deep aquifer. This mixing line indicated that some upward vertical leakage from the CI isotopically depleted paleogroundwater took place in some parts of CT aquifer. The second CT group constituted by the most enriched samples collected from the shallowest boreholes located far from the major faults. These samples scatter along a linear trend with a slope of 4, extending towards the point representing

the enriched weighted mean of the PQ groundwater. Consequently, this latter linear trend could be interpreted either as an evaporation line of the CT groundwater or as a mixing line between the CT and the PQ shallow aquifer groundwaters. However, it seemed more likely that the CT samples lying on this linear trend exhibited an apparent evaporation as they underwent some mixing with the groundwater of the PQ aquifer that is essentially recharged by the evaporated water of the irrigation return flow. Indeed, the excess of irrigation water fractionated at different rates in the irrigation channels and in the unsaturated zone, recharged the PQ shallow aquifer before reaching the CT intermediate aquifer and mixing with water from the regional groundwater flow system.

On the other hand, the CT groundwaters themselves could not be highly evaporated like they appeared in the  $\delta^2\text{H}/\delta^{18}\text{O}$  diagram for two simple reasons: (1) in most parts of the Djerid, the CT paleogroundwater is deeply confined to be exposed to the evaporation within the aquifer itself; (2) the regional present-day climatic conditions (very low rainfall amount and extremely high potential evapotranspiration) are unfavorable for an important modern recharge, which can give to the CT such evaporated signature.

#### *Spatial distribution of stable isotope*

The spatial distribution of  $\delta^{18}\text{O}$  (Fig. 14) and  $\delta^2\text{H}$  (not shown) contents in the groundwater of the CT aquifer provides other reliable information about the existence and the location of the likely interconnections between this intermediate aquifer on one hand; and the underlying CI and the overlying PQ aquifers on the other. It also permits

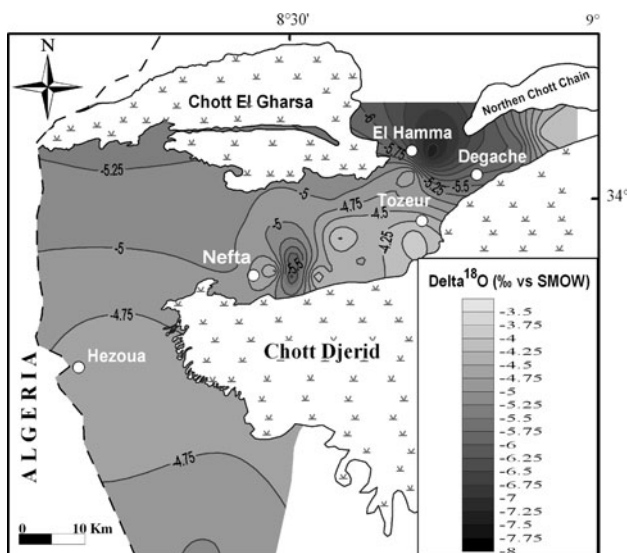


**Fig. 14** Spatial distribution of  $\delta^{18}\text{O}$  in the CT groundwaters

to elucidate the ambiguities about the possibility of modern the recharge of the CT aquifer.

In Fig. 14, the isotopically lowest groundwaters characterize the CT boreholes of Hamma and Ceddada regions (in the north of the basin), where the major faults reach their maximum depths. The relatively low oxygen-18 contents of these boreholes, already distinguished by the highest values of their well-head water temperatures, indicated the likely mixing of the CT groundwater with the isotopically depleted and geothermal waters of the CI deep aquifer, which migrate towards the CT by upward leakage through the deep parts of the major faults. On the other hand, the isotopically highest groundwaters distinguished particularly the oases domains of Nefta, Tozeur, and Dghoumes regions and the piedmont of the Dghoumes Mountain, representing the extremity of the northern Chotts range. These enriched groundwaters indicated essentially their mixing with relatively evaporated waters of the PQ shallow aquifer, recharged mainly in the oasis domains by return flow of irrigation water. However, the presence of some modern recharge in the CT aquifer, particularly in the piedmont of the Dghoumes Mountain, is not excluded.

#### **Summary and conclusion**

The hydrochemical characteristics of the CT groundwater in the study area comprise two main water types resulting from various processes in relation with water/rock interactions and mixing. The first  $\text{Na} > \text{Cl}$  water type highlighted the predominance of the halite dissolution. While, the second  $\text{Cl} > \text{SO}_4 > \text{Ca} > \text{Na}$  water type indicated the coexistence of the dissolution of both halite and gypsum, and the Ca–Na cation exchange and pyrite oxidation.

The faulted geological structure, whose main feature is the compartmentalization of the aquifer near the horst of the so-called “Tozeur ridge”, has played a major role in the appearance of some vertical leakage from the underlying deep CI aquifer. This upward leakage taking place along parts of the major faults of Tozeur uplift, particularly in Hamma and Ceddada regions, was evidenced by the relatively high groundwater head-well temperatures and the depleted stable isotope contents in these regions, and particularly by the mixing line appearing in the  $\delta^{18}\text{O}/\delta^2\text{H}$  diagram extended towards the point representing the weighted mean of the CI deep aquifer.

Another mixing effect, in relation with the downward leakage from the PQ shallow aquifer, influenced the CT groundwater composition. This mixing was enhanced by the return flow resulting from the long-term flood irrigation practices, which insured the recharge of the PQ aquifer in the oases domain. This leakage was confirmed through the spatial distribution of stable isotopes, which indicated that

the relatively enriched contents concentrated principally in the oasis domains, and through the  $\delta^{18}\text{O}/\delta^2\text{H}$  diagram that showed a mixing line with the PQ evaporated groundwater.

## References

- Abidi B (1993) Contribution à l'étude hydrogéologique de la région de Chott El Gharsa Nord. Doc Tech, DGRE, Tunis, 150 p
- Adams S, Titus R, Pietersen K, Tredoux G, Harris C (2001) Hydrochemical characteristics of aquifers near Sutherland in the Western Karoo, South Africa. *J Hydrol* 241:91–103
- Appelo CAJ, Postma D (1993) *Geochemistry, groundwater and pollution*, 2nd edn. Balkema, Rotterdam
- Bel F, Demargne F (1966) Etude géologique du Continental Terminal; DEC, ANRH, Alger, Algérie, 24 planches, 22 p
- Belloumi M, Matoussi M (2006) A stochastic frontier approach for measuring technical efficiencies of date farms in southern Tunisia. *Agric Resour Econ Rev* 35:285–298
- British Geological Survey (BGS) (1997) Recharge characteristics and ground water quality of the Grand Erg Occidental. Final Report EC (Avicenne) CT93AVI0015
- Chadha DK (1999) A proposed new diagram for geochemical classification of natural waters and interpretation of chemical data. *Hydrogeol J* 7:431–439
- Clark I, Fritz P (1997) *Environmental isotopes in hydrogeology*. Lewis Publishers, Boca Raton
- Coleman ML, Shepherd TJ, Durham JJ, Rouse JE, Moore GR (1982) Reduction of water with zinc for hydrogen isotope analysis. *Anal Chem* 54:993–995
- Coplen TB (1988) Normalization of oxygen and hydrogen isotope data. *Chem Geol* 72:293–297
- Cornet A (1964) Introduction à l'hydrogéologie saharienne. *Revue de Géographie, Physique et de Géologie Dynamique* (part 2), VI 1:5–72
- Craig H (1961) Isotopic variation in meteoric waters. *Science* 133:1702–1703
- Daoud D (1995) Caractérisation géochimique et isotopique des eaux souterraines et estimation du taux d'évaporation dans le bassin du Chott Chergui (zone semi-aride), Algérie. Thèse Doctorat Univ Paris-Sud, Orsay, p 256
- Edmunds W, Guendouz A, Mamou A, Moulla A, Shand P, Zouari K (2003) Groundwater evolution in the Continental Intercalaire aquifer of southern Algeria and Tunisia: trace element isotopic indicators. *Appl Geochem* 18:805–822
- Epstein S, Mayeda TK (1953) Variations of  $^{18}\text{O}$  content of waters from natural sources. *Geochim Cosmochim Acta* 4:213–224
- ERESS (1972) Etude des ressources en eau de Sahara septentrional. UNESCO, Paris
- Fontes JCh, Coque R, Dever L, Filly A, Mamou A (1983) Paléohydrologie isotopique de l'wadi el Akarit (Sud tunisien) au Pléistocène et à l'Holocène. *Pal Pal* 43:41–61
- Gonfiantini R, Dincer T, Derekoj AM (1974) Environmental isotope hydrology in the Hodna region, Algeria. In: *Isotope techniques in groundwater hydrology*. Proceeding symposium. IAEA, Vienna, pp 293–316
- Guendouz A, Moulla AS (1996) Drainance de la nappe profonde du Continental Intercalaire vers les aquifères superficiels à Ourgala: arguments isotopiques. Colloque International sur l'utilisation des techniques isotopiques dans les domaines des ressources en eau et en sol, Mahdia (Tunisie)
- Guendouz A, Moulla AS, Edmunds W, Shand P, Poole J, Zouari K, Mamou A (1997) Paleoclimatic information contained in groundwater of the Grand Erg Oriental. N. Africa. Proceeding symposium. IAEA, Vienna, p 349
- Horriche JF (2004) Contribution à l'analyse et à la rationalisation des réseaux piézométriques. Thèse Univ Tunis, Tunisia, p 260
- Jeribi L (1997) Contribution à la mise en évidence de l'alimentation de la nappe du Complexe Terminal à partir de la chaîne de Metlaoui-Gafsa. DEA Univ Tunis, Tunisia, p 96
- Kamel S (2007) Caractérisation hydrodynamique et géochimique des aquifères de Djérid (Sud-ouest Tunisien). Thèse Doctorat Univ Tunis, Tunisia, p 230
- Kamel S, Dassi L, Zaouri K, Abidi B (2005) Geochemical and isotopic investigation of the aquifer system in the Djerid-Nefzoua basin, southern Tunisia. *Env Geol* 49:59–170
- Mamou A (1990) Caractéristiques et évaluation des ressources en eau du sud tunisien. Thèse Doctorat Univ Paris-Sud, Orsay, p 320
- Moumni L (2001) La nappe des grès de Sidi Aïch ou Continental Intercalaire de Djérid Rap. Int. DGRE/OSS, p 43
- Pallas P (1980) Water resources of the Socialist People's Arab Libyan Republic. In: Salem MJ, Buswille MT (eds) *The geology of Libya*, vol II. ed. Academic Press, London
- Plummer LN, Prestemon E, Parkhurst DL (1992) An interactive code (netpath) for modelling net geochemical reactions along a flow path. *Techniques of water resources investigations of US geological survey*, pp 91–4078
- Rouatbi R (1967) Contribution à l'étude hydrogéologique du karst enterré de Gabès Sud. Thèse Doctorat Univ Montpellier, France
- Sadek MA, Abd El-Samie SG (2001) Pollution vulnerability of the Quaternary aquifer near Cairo, Egypt, as indicated by isotopes and hydrochemistry. *Hydrogeol J* 9:273–281
- SASS (2002) Le système aquifère du Sahara septentrional: une conscience de bassin. OSS, Vol et Annexes. OSS/SASS, Tunis
- Sonntag C, Klitzsch E, Lohnert EP, Munnich KO, Junghans C, Thorweihe U, Weistroffer K, Swailem FM (1978) Palaeoclimatic information from deuterium and oxygen-18 in carbon-14-dated north Saharian groundwaters. *Isotope Hydrology*. IAEA, Vienna, pp 569–581
- Tarki M (2008) Relations hydrauliques entre les aquifères superposés du bassin de Djérid: approches géochimique et isotopique. DEA, Univ Sfax, Tunisia, p 95
- Wallin B, Gaye C, Gourcy L, Aggarwal P (2005) Isotope methods for management of shared aquifers in Northern Africa. *Groundwater* 43:744–749
- Zargouni F (1986) Tectonique de l'Atlas méridional de Tunisie, évolution géométrique et cinématique des structures en zones de cisaillement. Thèse Doctorat Univ Louis Pasteur, Strasbourg, France
- Zouari K, Mamou A (1992) Les systèmes aquifères du Sud tunisien: Caractéristiques hydrochimiques et isotopiques, conditions de recharge et optimisation de la gestion. Actes du congrès International, Marrakech, pp 41–44
- Zouari K, Mamou A (1998) Etude isotopique et hydrochimique des systèmes multicouches de Gafsa et de Hajeb Aioun-Djilima (Tunisie Centrale). IAEA, Vienna, p 70
- Zouari K, Aranysoy JF, Mamou A, Fontes J CH (1985) Etude isotopique et géochimique des mouvements et de l'évolution des solutions de la zone aérée des sols sous climats semi-aride (Sud tunisien). In: *Stable and radioactive isotopes in the study of the unsaturated soil zone*. IAEA, Vienna, pp 121–144